792
NACA TN 2391

TECH LIBRARY KAFB, NM
0065723

NATIONAL ADVISORY COMMITTEE FOR AERONAUTICS

TECHNICAL NOTE 2391

FURTHER COMPARISONS OF THEORETICAL AND EXPERIMENTAL LIFT AND PRESSURE DISTRIBUTIONS ON AIRFOILS IN CASCADE AT LOW-SUBSONIC SPEED

By S. Katzoff and Margery E. Hannah

Langley Aeronautical Laboratory
Langley Field, Va.

NACA
Washington
August 1951

AFWL
TECHNICAL LIBRARY
AFL 2811

TECH LIBRARY KAFB, NM
0065723

NATIONAL ADVISORY COMMITTEE FOR AERONAUTICS

TECHNICAL NOTE 2391

FURTHER COMPARISONS OF THEORETICAL AND EXPERIMENTAL LIFT AND PRESSURE DISTRIBUTIONS ON AIRFOILS IN CASCADE AT LOW-SUBSONIC SPEED

By S. Katzoff and Margery E. Hannah

SUMMARY

Comparisons of theoretical and experimental lift coefficients and pressure distributions were made for five compressor-type cascades of highly cambered NACA 6-series airfoils. The experimental lift coefficients, which were between 0.81 and 0.96, were 0.18 to 0.41 less than the theoretical values for the same mean-flow direction. When the theoretical lift coefficients were made equal to the experimental lift coefficients by putting the circulation equal to the required value, the Kutta condition being neglected, the agreements between the two pressure distributions were very close, except for the configurations with the highest pressure rise across the cascade (59 and 64 percent of the upstream dynamic pressure). Interesting irregularities in the experimental pressure distributions, not present in the calculated distributions, were found to be caused by localized regions of laminar separation.

The experimental data used in these comparisons were obtained by the newer technique described in NACA TN 2028. The present paper is thus to some extent a revision of an earlier paper, NACA TN 1376, where substantially poorer comparisons were found for data obtained by the older techniques.

INTRODUCTION

In reference 1 several comparisons were made between theoretical lift coefficients and pressure distributions on airfoils in cascade and the corresponding experimental lift coefficients and pressure distributions, reported in references 2 and 3. As with isolated airfoils, the experimental lift coefficients were always less than the theoretical lift coefficients; however, the differences were found to be remarkably large, especially for compressor blading with large turning angles. Furthermore, as is also true of isolated airfoils, a more or less

acceptable agreement between the pressure distributions could be obtained if the circulation was adjusted to correspond to the experimental lift coefficient, either with superposition of sufficient negative camber, as in reference 4, so that the Kutta condition at the trailing edge would still be obeyed, or with simple disregard of the Kutta condition.

As was also pointed out in reference 1, however, certain disturbing inconsistencies existed in many of the experimental cascade data. In particular, both the blade lift and the pressure rise were too small to correspond to the measured turning angle, apparently because of large three-dimensional effects resulting from the wall boundary layer. Furthermore, in tests of an actual compressor it was found that the pressure rise did correspond to the turning angle, from which it was concluded that the lift on the rotating blades was probably much higher than that on the cascade blades. In view of these and other indications (see reference 5) that the measured pressures in the cascade did not correspond accurately either to two-dimensional cascade flow or to flow in the actual compressor, the significance of the comparisons for these cases became very uncertain and no more comparisons were attempted.

More recently (reference 5), the Langley Laboratory has considerably improved the experimental technique, mainly by the use of continuous boundary-layer suction on the walls at the ends of the blades, so that the data now being obtained appear to correspond to practically two-dimensional flow. Accordingly, the question of the relation between theoretical and experimental lift and pressure distribution has been reopened and several calculations have been made for comparison with the newer data. The comparisons, which were mainly very satisfactory, are reported in the present paper, not only to supplement the discussion in reference 5 but also to provide an extension and revision of reference 1.

SYMBOLS

V	airspeed
q	dynamic pressure
α	angle of attack, measured with respect to chord line
$\Delta\alpha$	assumed change in α, used to improve agreement between experimental and calculated velocity distributions
β	angle between flow direction and normal to cascade

σ	solidity
θ	turning angle
c_l	lift coefficient
c_{d_2}	drag coefficient determined from wake surveys by the Jones drag equation, with downstream static pressure considered as free-stream pressure

Subscripts:

1	upstream
2	downstream
m	mean
a	axial
th	theoretical
exp	experimental
red	reduced

REVIEW OF BASIC CONCEPTS AND PROCEDURES

Angles and velocities.- As explained in reference 5, the suction on the wall of the cascade tunnel is adjusted until the pressure rise across the cascade corresponds to the turning angle, with allowance for the displacement thickness of the blade wake. (The data are subsequently also checked for other criteria of two-dimensionality, such as agreement between the force on the blade and the momentum and pressure changes across the cascade.) In the corresponding velocity diagram (fig. 1) the downstream axial velocity of the main flow between the wakes V_{a_2} slightly exceeds the upstream axial velocity V_{a_1} because of this effective reduction of flow area by the wake. The upstream total velocity V_1, the inlet-air angle β_1, and the turning angle θ are defined in the usual manner. The downstream velocity V_2 is that of the main flow between the wakes rather than the average velocity of all the downstream air, and the angle β_2 gives its direction. The relative pressure rise is $1 - \left(\frac{V_2}{V_1}\right)^2$.

In the theoretical calculations, only incompressible potential flow is considered, in which, for example, $V_{a_2} = V_{a_1}$; so that the question immediately arises as to how to define the theoretical flow with which the experiment is to be compared (for example, should its axial component be taken as V_{a_1} or as V_{a_2}?). Since no especially rational answer presented itself, the mean-flow velocity V_m or the vector mean of the upstream and downstream velocities in the potential flow, which is a basic parameter in the present calculation method, was defined as the vector mean of the experimental velocities V_1 and V_2. (See fig. 1.) The angle that the chord line makes with this mean velocity is denoted α_m.

Calculation method.- The calculations were made according to the method of reference 6, in which attention is fixed on one airfoil (called the central airfoil) of the cascade, and the lift and the velocity distribution on this airfoil are each considered to be the sum of two components: that due to straight uniform flow of velocity V_m, making an angle α_m with the chord line (see fig. 1), and that due to the interference flow caused by the presence of all the other airfoils (called the external airfoils) of the infinite cascade. For convenience, the interference flow is evaluated in two parts: that due to the sources and sinks that represent the thickness distribution along the interfering (external) airfoils and that due to the vortices that represent the lift distribution along the external airfoils. Since the external airfoils must actually be similar to the central airfoil, the lift and the velocity distribution of the central airfoil due to its presence in this combined field must, in the final solution, be the same as the lift and the velocity distribution of the external airfoils. This solution is found by an iteration method that converges very rapidly.

Because of viscosity, the experimental lift of the airfoil for the given mean flow V_m is always less than the theoretical lift. As in reference 1, the purpose of the present study is not only to evaluate this difference but also to determine whether, if the lift of the airfoil in potential flow is made equal to the experimental lift, the corresponding theoretical pressure distribution could then match the experimental pressure distribution. As previously mentioned, two

methods were used in reference 1 for calculating pressure distribution to correspond to the reduced lift. In one, the Kutta condition is disregarded and the lift adjustment is obtained by merely reducing the circulation to the desired value. The rear stagnation point is thereby moved to the upper surface of the airfoil, and the calculated velocity distributions on the upper and lower surfaces show a characteristic crossing-over slightly ahead of the trailing edge. In the other method, based on that of reference 4, the airfoil is assumed to be distorted, according to a specified procedure, so that the lift reduction is attained without disregarding the Kutta condition.

In the present studies the distortion method, applied as in reference 1, was found to yield generally less satisfactory comparisons with experiment than did the simple adjustment of the circulation. Accordingly, only one result derived by the distortion method is shown. In some cases it was found that assuming the angle of attack of the blade relative to the mean flow to be somewhat less than the true angle (or, at least, the experimentally determined angle) resulted in improved agreement between the calculated and the measured results. The results of these modified calculations have been shown for these cases. Some discussion of the possible significance of these assumed reductions in angle of attack is given in a subsequent section.

COMPARISONS OF CALCULATED AND EXPERIMENTAL RESULTS

Experimental data.- The five experimental pressure distributions used for the present analyses were obtained by the Cascade Aerodynamics Section of the Langley Aeronautical Laboratory. They have not previously been published. The examples were selected to include inlet-air angles of 45° and 60° and to cover the higher range of lift coefficients. Three of the cascades used the NACA 65-(12)10 airfoil section, one used the NACA 65-(18)10 airfoil section, and the fifth used a special section, designated the NACA 65-(12A)10 airfoil section, which is highly cambered toward the rear. The solidity was 1.0 for three cases and 1.5 for the other two. The inlet speeds were of the order of 95 feet per second, so that the flow was essentially incompressible. This speed and the 5-inch blade chord correspond to a Reynolds number of about 250,000.

Detailed discussion of the examples is given in the succeeding sections. The basic experimental data and the comparisons with calculated results are summarized in the following table:

Example	Figure	NACA airfoil	σ	β_1 (deg)	θ (deg)	α_1 (deg)	α_m (deg)	Pressure rise (percent q_1)	c_{d_2}	c_{l_m}		$\Delta\alpha_m$ (deg)	Pressure-distribution comparison
										Theoretical	Experimental		
1	2	65-(12)10	1.0	45	19.6	12.1	3.4	36	0.025	1.00	0.82	0	Good
2	3	65-(12A)10	1.0	45	17.9	9.8	1.8	34	------	1.22	.81	-.5	Good
3	4	65-(12)10	1.0	60	18.6	14.1	6.5	52	.034	1.31	.96	-1.2	Good
4	5	65-(12)10	1.5	60	24.6	18.1	8.6	59	.030	1.07	.82	-1.1	Satisfactory
5	6	65-(18)10	1.5	60	29.8	21.0	10.1	64	.053	1.32	.96	-----	Satisfactory

Example 1: NACA 65-(12)10 airfoil, $\beta_1 = 45^\circ$, $\sigma = 1.0$.- In figure 2 are shown the comparisons for a cascade of NACA 65-(12)10 airfoils at unit solidity and an inlet-air angle of 45°. For the given mean-flow direction, the theory indicated a lift coefficient of 1.00 and a velocity distribution as indicated by the solid line. Neglecting the Kutta condition and reducing the circulation to correspond to the measured lift coefficient of 0.82 resulted in the velocity distribution shown by the dashed line. The agreement with the experimental points is very close, in striking contrast with the comparisons of reference 1. Furthermore, the difference between the experimental and the unadjusted theoretical lift coefficients is much smaller than the differences found in reference 1.

Some slight irregularities of the experimental points toward the rear on both the upper and lower surfaces may be noted; these irregularities are discussed with the next two examples, for which they are much more pronounced. Also of interest is the pronounced peak velocity shown by the theoretical curve for the lower surface at the nose. No pressure orifices were installed in this region of the airfoils, so the existence of this peak is not verified experimentally. It is present, however, on most of the calculated velocity distributions for this airfoil at conditions that would otherwise be classed as approximately "design conditions."

If more detailed measurements verify its existence some slight redesign of the airfoil in this region or a slight increase in angle of attack might be desirable in order to eliminate the peak; however, it is not obvious that the peak would do any appreciable harm.

Example 2: NACA 65-(12A)10 airfoil, $\beta_1 = 45^\circ$, $\sigma = 1.0$.- The NACA 65-(12A)10 is a special airfoil having the NACA 65-010 thickness distribution but a mean line that is highly cambered toward the rear (see fig. 3). It was tested at unit solidity and with an inlet-air angle β_1 of 45°. For the experimentally determined mean-flow direction, the theory indicated a lift coefficient of 1.22, compared with the experimental lift coefficient of 0.81. The fact that the difference between theoretical and experimental lift coefficients for this case was more than twice that of the preceding example, although the flow geometry and the pressure rise across the cascade were nearly the same, is presumably due to the very high camber at the trailing edge of this airfoil. Adjusting the circulation to correspond to the experimental lift coefficient resulted in the dashed curve of figure 3. Again, the agreement with experiment is very close, although it could be further improved by reducing the angle of attack by 0.5° (long-and-short-dash line).

Examination of the experimental velocity distribution on the upper surface shows a definite bump at about the 80-percent-chord station, whereas the theoretical curve is quite smooth in this region. Careful study failed to show any experimental or analytical inaccuracy or any inaccuracy in airfoil contour, and the cause of the bump was finally ascertained to be an effective local change in airfoil contour caused by a localized region of laminar separation (or laminar-separation bubble) such as described in reference 7. Because of the low Reynolds number of the tests (about 250,000) and the low stream turbulence, the boundary layer generally remains laminar until it separates (where the local velocity has dropped several percent below the peak velocity); at this point a low laminar separation bubble is formed (the size of which depends on the Reynolds number), toward the rear of which the boundary layer becomes turbulent and reattaches itself to the surface.

Studies by the Langley Cascade Aerodynamics Section showed that an increased Reynolds number, a fine wire stretched across the tunnel just upstream of the blade (to create turbulence in the air stream), or roughness toward the nose of the blade could induce transition at or ahead of the laminar separation point and eliminate both the bubble and the corresponding bump in the pressure distribution. Since corresponding (unpublished) pressure distributions measured on the blades of a rotating compressor failed to show the bump, it may be assumed that the compressor flow is sufficiently turbulent to cause transition ahead of what would otherwise be the laminar separation point. It might

accordingly seem desirable that cascade data be obtained under corresponding flow conditions. The tests with artificially induced transition did not show, however, any very consistent effect on lift or drag; also, compressor-flow data seem to be in satisfactory agreement with the cascade data, at least for the types of blading used in the work of reference 5.

The slight irregularities noted in figure 2 may also be associated with small separation bubbles. Some of the subsequently presented data show very pronounced bumps; however, they are not always present when the pressure distributions indicate that laminar separation could exist, for which cases, presumably, experimental conditions were such as to cause previous transition. With regard to the indications of laminar separation on the pressure surface of the airfoils in figures 2 and 4, the question may arise as to whether the previously mentioned pressure peak that may possibly exist at the airfoil nose would not cause immediate transition at the nose on the pressure surface. In reference 8, however, it was shown that at very low boundary-layer Reynolds numbers a laminar boundary layer can separate and reattach as a laminar boundary layer; accordingly, no definite conclusion can be drawn.

Example 3: NACA 65-(12)10 airfoil, $\beta_1 = 60^\circ$, $\sigma = 1.0$.- In figure 4 are shown comparisons for the NACA 65-(12)10 airfoil at unit solidity and an inlet-air angle of 60°. For the given mean-flow direction, the theory indicated a lift coefficient of 1.31 and a velocity distribution as indicated in figure 4. Reducing the circulation to provide the experimental lift coefficient of 0.96 resulted in the dashed curve of the figure, which might be considered in quite satisfactory agreement with the experimental curve. If, in addition, the mean angle of attack is reduced from 6.5° to 5.3°, almost perfect agreement results. Pronounced irregularities in the experimental distributions at about 60 percent chord on the upper surface and 70 percent chord on the lower surface are again attributable to laminar-separation bubbles at these points.

The fact that the difference between experimental and theoretical lift coefficients in this case is twice that of example 1, although the airfoils are the same, is to be ascribed to the higher pressure rise across the cascade and the corresponding thickening of the boundary layer over the trailing edge. In example 1, the pressure rise across the cascade was 36 percent of the upstream dynamic pressure, whereas in the present example, it was 52 percent.

Example 4: NACA 65-(12)10 airfoil, $\beta_1 = 60^\circ$, $\sigma = 1.5$.- In figure 5 are shown results for an arrangement similar to that of

example 3, except that the solidity is increased to 1.5. For the given mean-flow direction, the theory indicated a lift coefficient of 1.07, whereas the experimental lift coefficient was 0.82. Reducing the circulation to the experimental value gave a calculated velocity distribution as shown by the dashed line of figure 5. Reducing the angle of attack from 8.6° to 7.5° gave a velocity distribution as shown by the long-and-short-dash line. The agreement between this curve and the experimental points is satisfactory but not so close as the agreements shown in the preceding three cases.

This example may appear somewhat puzzling since, although the pressure rise across the cascade - 59 percent of the upstream dynamic pressure - was even larger than that of the previous example, the difference between the theoretical and experimental lift coefficients was only 0.25, compared with 0.35 for the previous example. Some further discussion of this point is given subsequently.

Example 5: NACA 65-(18)10 airfoil, $\beta_1 = 60^\circ$, $\sigma = 1.5$.- Figure 6 shows comparisons for an arrangement similar to example 4 except that the airfoil is more highly cambered. For this case the relative pressure rise across the cascade was the highest of those studied - 64 percent of the upstream dynamic pressure - and the comparison between theoretical and experimental velocity distributions was correspondingly the poorest of the present group, although it is considered satisfactory. For the given mean flow, the theory indicated a lift coefficient of 1.32, compared with the experimental value of 0.96. Reducing the circulation to the experimental value gave the dashed-line curve of figure 6. The agreement is seen to be quite close over most of the lower surface but not very close over the upper surface. Reducing the mean angle of attack from 10.1° to 8.0° (the long-and-short-dash curve of fig. 6) showed no clear improvement; it resulted in a somewhat closer agreement over the nose of the airfoil but a poorer agreement toward the rear. The rather violent pressure rise between 40 and 50 percent chord on this surface suggests the possibility that the agreement with theory might be considerably affected, perhaps improved, by sufficient roughness or turbulence to reduce or eliminate the laminar-separation bubble at that location.

The shape of the experimental velocity distribution toward the rear of the upper surface indicates that the boundary layer is very thick and either separated or on the verge of separation in this region. Presumably such conditions would result not only in a large loss of lift but also in a large effective distortion of the profile. In order to determine whether the distortion method used in reference 1 might improve the agreement for this case, calculations were also performed by that method. The resulting curve is seen to be appreciably different from that obtained by simply reducing the circulation without regard to the Kutta condition, although the over-all agreement is not closer.

Summary of comparisons.- Of the five comparisons that have been made, the first three were very close, the fourth was fairly close over the suction surface but less satisfactory over the pressure surface, and the fifth was satisfactory over the pressure surface but much less satisfactory over the upper surface. The combination of high lift coefficient and high pressure rise in the last two cases was presumably the basic cause of the disagreements. The angle-of-attack reduction required for best agreement (0°, 0.5°, 1.2°, 1.1° for the first four cases) is also roughly in the order of increasing pressure rise. In general, then, it appears that for configurations and conditions similar to the types discussed:

(a) The lift coefficient of an airfoil in cascade may be less than the theoretical lift coefficient (Kutta condition satisfied) by about 0.2 to 0.4, depending on such parameters as the inlet-air angle, the turning angle, the lift coefficient, the pressure rise across the cascade, the solidity, and the degree of camber near the trailing edge (these parameters, however, are not all independent)

(b) Forcing the theoretical lift coefficient to equal the experimental lift coefficient by simply adjusting the circulation to the required value, without regard to the Kutta condition, will provide generally adequate agreement between theoretical and experimental pressure distributions

(c) Assuming a small reduction in the angle of attack, of the order of 1°, may improve the agreement when the pressure rise is high

FURTHER DISCUSSION OF ANALYTICAL METHODS

The present section contains various additional remarks intended in part to help justify the methods employed and in part to contribute present experience to any workers wishing to make similar calculations. With regard to the methods of improving the agreement, however, it is very likely that the experimental cascade aerodynamicist, cognizant of the many experimental difficulties in his work, may be quite satisfied with the velocity distributions computed by merely neglecting the Kutta condition and may consider that further refinements and discussion of such refinements are unwarranted and perhaps would be inapplicable to some other set of experimental cascade data. The only direct evidence against such a viewpoint is the apparently systematic variation of the angle reduction with pressure rise, although the possibility still exists that, for example, the experimental determination of flow angles contains a small systematic error that increases with pressure rise.

Angle-of-attack reduction.- The improved agreement resulting from a small angle-of-attack reduction must be at least partly due to the fact that the boundary layer on the upper surface thickens more rapidly than does that on the lower surface so that a corresponding reduction in the effective angle of attack of the mean camber line results. Actually, since the boundary layer on the suction side thickens more and more rapidly as the trailing edge is approached, some effective reduction of the trailing-edge camber is probably also included. No data are available, however, by which these effects may be evaluated for the present examples.

In addition, if the flow was not actually two-dimensional, so that the lift decreased toward the wall, the trailing vortices would induce a downflow that would effectively reduce the angle of attack. It should also be noted that, since the presence of the viscous wake was taken into account only by arbitrarily defining V_m as the vector mean of V_1 and V_2, the need for some further patching of the calculation method when the wake becomes thick should not be unexpected.

Effect of wall suction slots.- In addition to the porous walls at the test section itself, the cascade tunnel contains a pair of wall suction slots located upstream of the cascade, the purpose of which is to remove most of the wall boundary layer before it reaches the test section (see fig. 7 of reference 5). Whereas in the older work these slots were of the scoop type, so that they effectively skimmed off the boundary layer, the present slots are flush with the wall surface so that in the process of removing the boundary layer they must distort the main flow to some extent. In order to obtain a rough estimate of the distortion that is so created, the slots were assumed to be represented by uniform sink distributions and the field of these distributions (and of their doubly periodic array of images) was calculated along the midspan chord of the center airfoil for a configuration with a 60° inlet-air angle. For a typical suction quantity (for both slots) of 4 percent of the tunnel flow the induced angularity was found to be about 0.5° near the leading edge and about 0.2° near the trailing edge, with its direction such as to increase the blade angle of attack. Thus the effect is small and in the wrong direction to justify the angle-of-attack changes that were assumed in order to improve the agreement between calculated and experimental velocity distributions.

Difference between experimental lift and theoretical lift (Kutta condition satisfied).- In example 4 it was noted that the experimental lift coefficient was only 0.25 less than the theoretical lift coefficient, whereas the difference was 0.35 in example 3, which concerned the same airfoil with a lower pressure rise. It must be realized,

however, that this difference is not a direct, or unique, measure of the viscosity effect because it is partly involved with the slope of the lift curve in cascade, which depends on the configuration. On the basis of the concepts underlying the present calculation method, the matter could be discussed as follows: For example 3, the theoretical lift coefficient, with the Kutta condition satisfied, is 1.31; that is, when the external airfoils (see "Review of Basic Concepts and Procedures") have a lift coefficient of 1.31 and the correct velocity distribution, the central airfoil will have this same lift coefficient and velocity distribution. If, however, the external airfoils have only the experimental lift coefficient of 0.96, the interference will be reduced and the "theoretical" lift coefficient of the central airfoil, with the Kutta condition satisfied, will be 1.39. Since the experimental value is only 0.96, one may say that viscosity has reduced the lift coefficient by 0.43 (or 31 percent of 1.39) for this case, instead of 0.35 as previously mentioned. Similarly, for example 4, when the external airfoils have the experimental lift coefficient of 0.82, the theoretical lift on the central airfoil, with the Kutta condition satisfied, is 1.28, which differs from the experimental value by 0.46 (or 36 percent of 1.28). By such reasoning one may argue that the viscosity effect is greater for example 4 than for example 3. Furthermore, since the mean velocities near the trailing edge are appreciably less in example 4 than in example 3 (corresponding to the greater pressure rise), the displacement of the rear stagnation point is somewhat greater than the ratio of 0.46 to 0.43.

In an interesting effort to achieve the full theoretical lift, Mr. W. M. Schultz of the Langley Cascade Aerodynamics Section tested a cascade of NACA 65-(12)10 airfoils with boundary-layer control on the blades themselves. The blades were hollow and covered with perforated brass sheet that contained about 600 holes per square inch and which was hammered to reduce the hole size and provide a convenient pressure drop. Suction through the hollow interior provided continuous boundary-layer removal over the entire blade except for the leading- and trailing-edge sections where the blade was made solid in order to provide the necessary mechanical strength. Since the cascade had the same solidity and inlet-air angle as example 3 and had nearly the same blade setting, the pressure distributions for the two cases are compared in figure 7 and the data are compared in the following table:

Airfoil	θ (deg)	α_1 (deg)	α_m (deg)	Pressure rise (percent q_1)	c_{d_2}	c_{l_m}	
						Theoretical	Experimental
Solid	18.6	14.1	6.5	52	0.034	1.31	0.96
Porous	21.1	14.5	6.3	59	.0095	1.27	1.14

The theoretical c_{l_m} is 1.31 for example 3 but is reduced to 1.27 for the porous airfoil because of the differences of 0.2° in α_m and of 0.4° in the blade setting. The experimental c_{l_m} for the porous airfoil was only 1.14, so that a difference of 0.13 between theoretical and experimental lift coefficients for the porous airfoil still remains. It will be noted, however, that the wake was not at all negligible for this case; the indicated value of c_{d_2} was 0.0095, which is more than one-fourth the value of 0.034 for example 3.

The conformal transformation of a highly cambered airfoil to a circle.- In the conformal transformation of an airfoil to a circle by Theodorsen's method (reference 9), the base line in the transformation to the near circle is taken as the line that connects the point midway between the nose and its center of curvature with the point midway between the trailing edge and its center of curvature. The near circle will then have no sharp irregularities in the regions corresponding to the leading and trailing edges. For highly cambered airfoils, such as those of the present study, it must be emphasized that the airfoil nose must here be defined not as the farthest forward point of the airfoil (the nominal leading edge) but as the tip of the mean camber line, where the surface curvature is a maximum. The correct location of the base line, or reference axis, is illustrated in figure 8.

Another problem that arises in the conformal transformation of a highly cambered airfoil results from the large distance between the origin, or center of coordinates, and the approximate center of the near circle. Although two or three iterations may suffice for an accurate transformation of such a near circle to a circle about the origin, moving the origin to the approximate center of the near circle, as suggested in reference 9, is a preferable procedure. A computational procedure for changing the θ and ψ coordinates of points on the near circle to, say, θ_1 and ψ_1 corresponding to the new origin is as follows (familiarity with the concepts and nomenclature of reference 9 will be assumed in the present section):

Let the new origin be at point (a,b) relative to the original origin. Then the abscissa and ordinate of a point on the near circle relative to the new origin are $e^{\psi}\cos\theta - a$ and $e^{\psi}\sin\theta - b$. The angle θ_1 is thus $\tan^{-1}\dfrac{e^{\psi}\sin\theta - b}{e^{\psi}\cos\theta - a}$ and ψ_1 is determined from

$$e^{\psi_1} = \sqrt{\left(e^{\psi}\sin\theta - b\right)^2 + \left(e^{\psi}\cos\theta - a\right)^2}$$

In the final determination of the velocities on the airfoil, it must also be noted that the factor k at every point includes a new term, $e^{\psi-\psi_1}$. That is,

$$k = \frac{\left[1 + \epsilon'(\theta_1)\right] e^{\psi_0} e^{\psi-\psi_1}}{\sqrt{\left(\sin^2\theta + \sinh^2\psi\right)\left\{1 + \left[\psi'_1(\theta_1)\right]^2\right\}}}$$

Computational accuracy.- In reference 1 it was noted that the calculation for the turbine-blade cascade, where the solidity was 1.8 and the lift coefficient was 2.5, converged comparatively poorly and was relatively inaccurate because of the large interference potentials resulting from the high solidity and high lift coefficient. It is considered of interest in this connection to point out that in the least favorable of the present examples, in which the solidity was 1.5 and the lift coefficient was about 1.3, no such basic difficulties were experienced, although it was observed that convergence was indeed somewhat slower than for the unit-solidity cascades. Because of this slower convergence, high accuracy was not attempted for the theoretical curves of figures 5 and 6; the necessary labor would not have been justified in view of the fact that the discrepancy with experiment was in any case very much larger than the inaccuracy of the theoretical curve.

CONCLUSIONS

Comparisons have been made between calculated and experimental lift and velocity distributions for five compressor-type cascades of highly cambered NACA 6-series airfoils. The study is essentially a revision of NACA TN 1376, where a similar study showed generally poor comparisons.

The present study, the experimental data for which were obtained by the improved techniques of NACA TN 2028, indicates that:

1. For a given mean-flow direction, the experimental lift coefficient is less than the theoretical by reasonable amounts. For the present examples, in which the lift coefficients were between 0.81 and 0.96 and the values of pressure rise were between 34 and 64 percent of the upstream dynamic pressure, the differences were between 0.18 and 0.41, where the largest difference occurred for a special airfoil with very high trailing-edge camber.

2. The pressure distribution calculated by neglecting the Kutta condition and putting the circulation equal to the experimental value is in good agreement with the experimental pressure distribution provided the pressure rise is not so high that the airfoil boundary layer separates or approaches separation. Under such conditions, accordingly, the pressure distribution can be calculated with satisfactory accuracy when the cascade geometry and the incoming and outgoing flow directions are given. Incidentally, the observed agreement provides additional evidence of the validity of the experimental technique.

3. Pressure distributions obtained in a low-turbulence air stream at typical cascade-test Reynolds numbers may be characterized by the presence of bumps due to laminar-separation bubbles. This phenomenon appears not to exist on the blades of an actual compressor because of early transition. The basic cascade data, however, remain generally valid since the corresponding differences in the basic blade characteristics are probably negligible for most cases.

Langley Aeronautical Laboratory
National Advisory Committee for Aeronautics
Langley Field, Va., May 22, 1951

REFERENCES

1. Katzoff, S., Bogdonoff, Harriet E., and Boyet, Howard: Comparisons of Theoretical and Experimental Lift and Pressure Distributions on Airfoils in Cascade. NACA TN 1376, 1947.

2. Bogdonoff, Seymour M., and Bogdonoff, Harriet E.: Blade Design Data for Axial-Flow Fans and Compressors. NACA ACR L5F07a, 1945.

3. Zimney, Charles M., and Lappi, Viola M.: Data for Design of Entrance Vanes from Two-Dimensional Tests of Airfoils in Cascade. NACA ACR L5G18, 1945.

4. Pinkerton, Robert M.: Calculated and Measured Pressure Distributions over the Midspan Section of the N.A.C.A. 4412 Airfoil. NACA Rep. 563, 1936.

5. Erwin, John R., and Emery, James C.: Effect of Tunnel Configuration and Testing Technique on Cascade Performance. NACA TN 2028, 1950.

6. Katzoff, S., Finn, Robert S., and Laurence, James C.: Interference Method for Obtaining the Potential Flow past an Arbitrary Cascade of Airfoils. NACA Rep. 879, 1947. (Formerly NACA TN 1252.)

7. Gault, Donald E.: Boundary Layer and Stalling Characteristics of the NACA 63-009 Airfoil Section. NACA TN 1894, 1949.

8. Liepmann, Hans W., and Fila, Gertrude H.: Investigation of Effects of Surface Temperature and Single Roughness Elements on Boundary-Layer Transition. NACA Rep. 890, 1947.

9. Theodorsen, T., and Garrick, I. E.: General Potential Theory of Arbitrary Wing Sections. NACA Rep. 452, 1933.

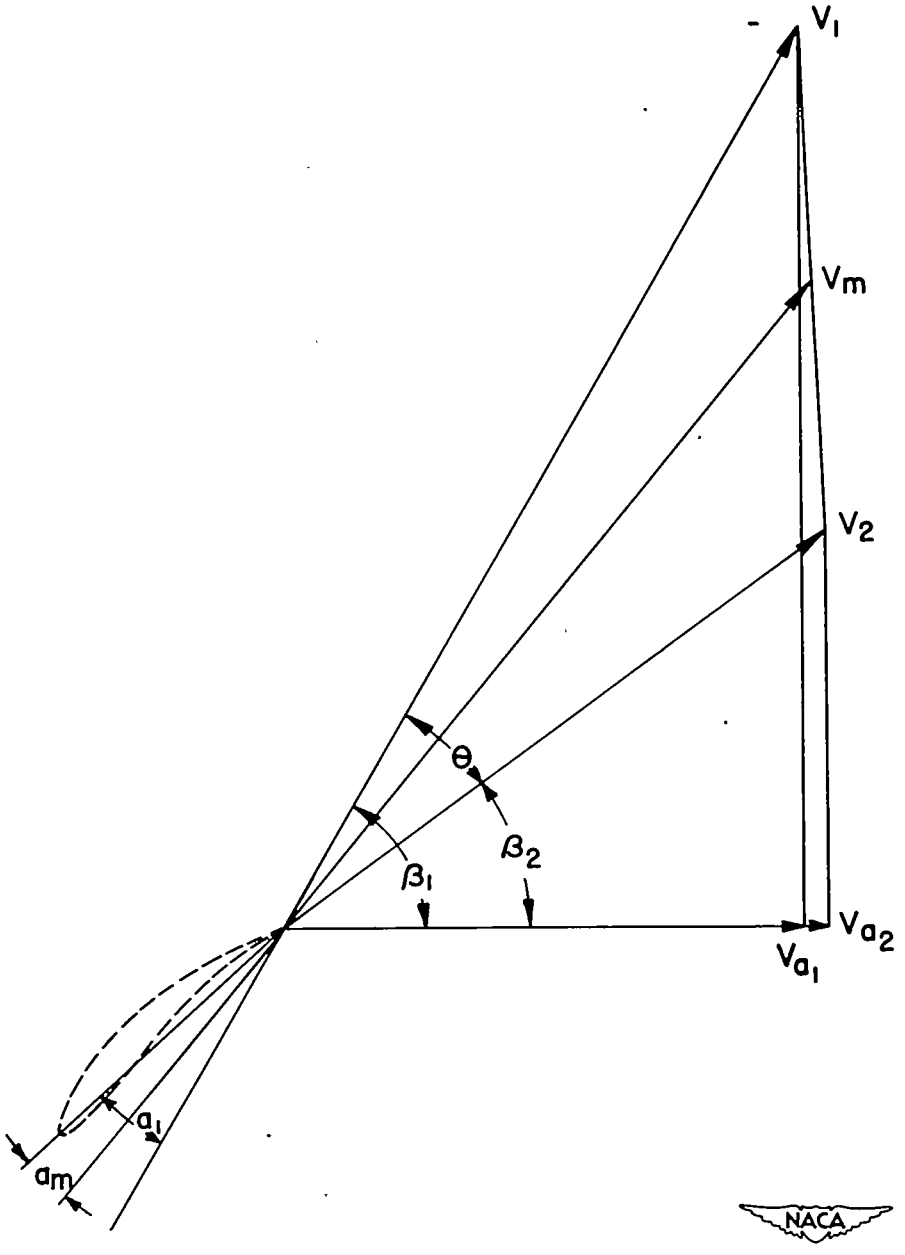

Figure 1.- Definitions of velocities and angles.

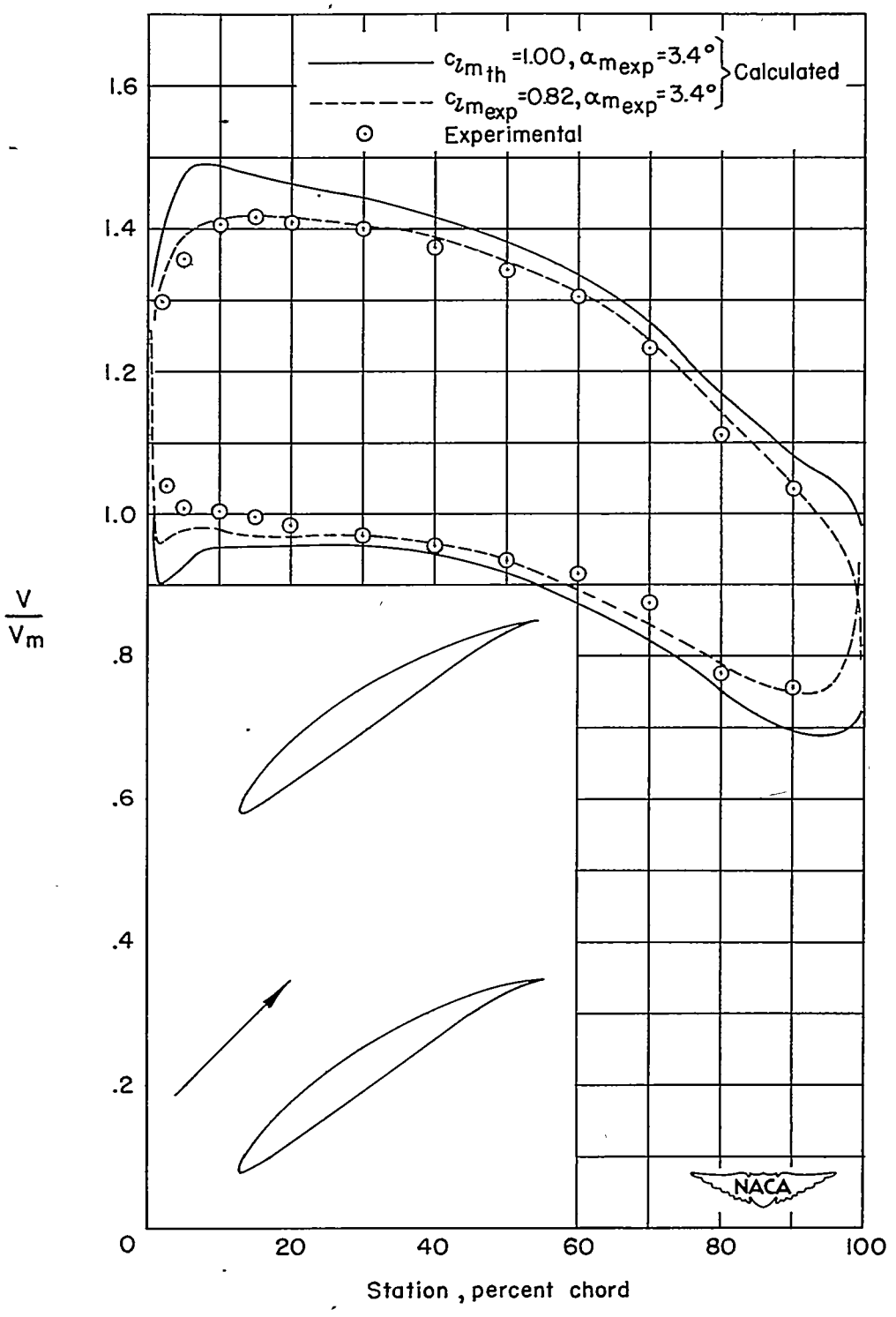

Figure 2.- Comparison of experimental and theoretical velocity distribution on airfoil in cascade. NACA 65-(12)10 airfoil; $\beta_1 = 45^\circ$; $\alpha_1 = 12.1^\circ$; $\alpha_m = 3.4^\circ$; $\theta = 19.6^\circ$; $\sigma = 1.0$.

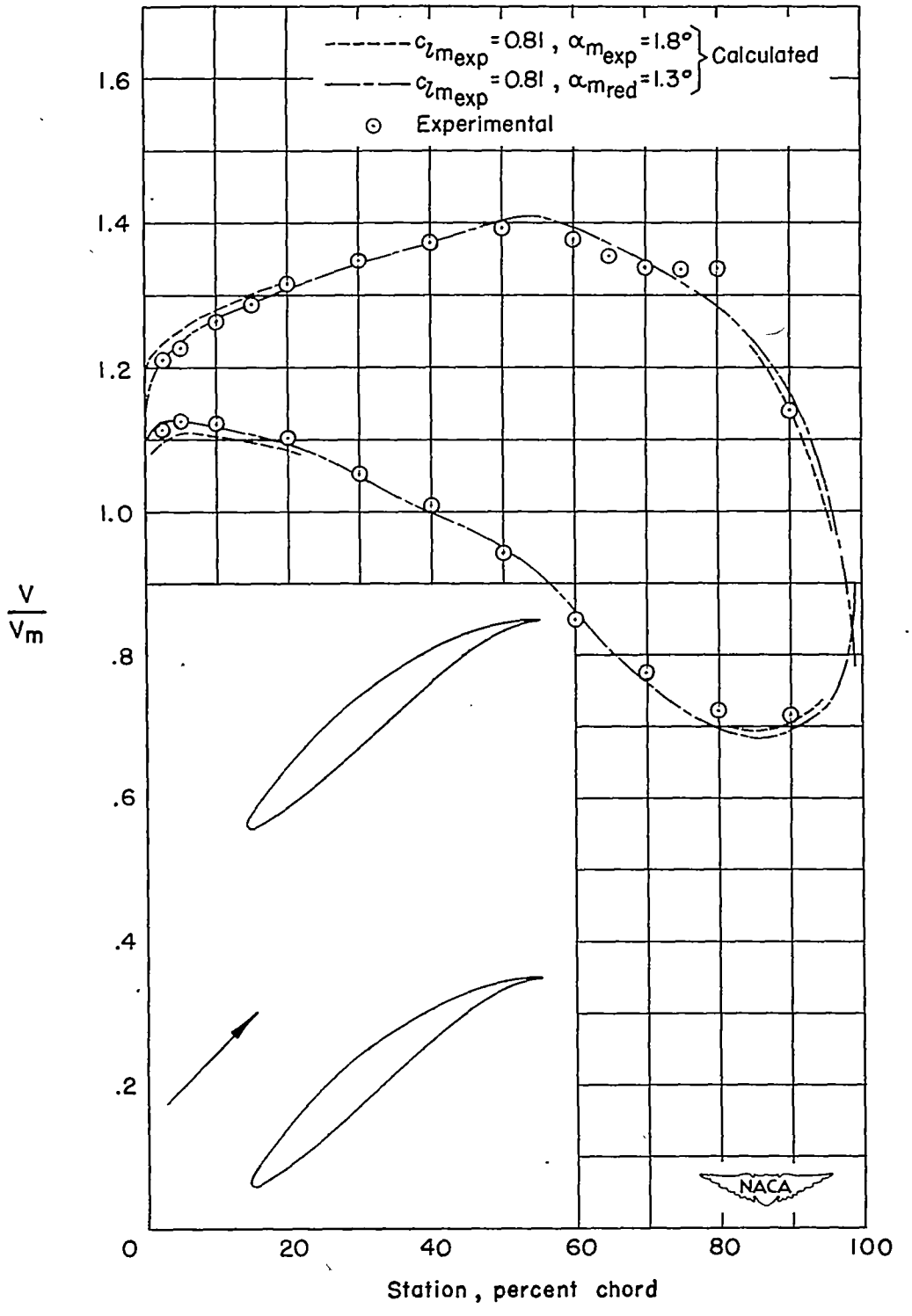

Figure 3.- Comparison of experimental and theoretical velocity distribution on airfoil in cascade. NACA 65-(12A)10 airfoil; $\beta_1 = 45°$; $\alpha_1 = 9.8°$; $\alpha_m = 1.8°$; $\theta = 17.9°$; $\sigma = 1.0$.

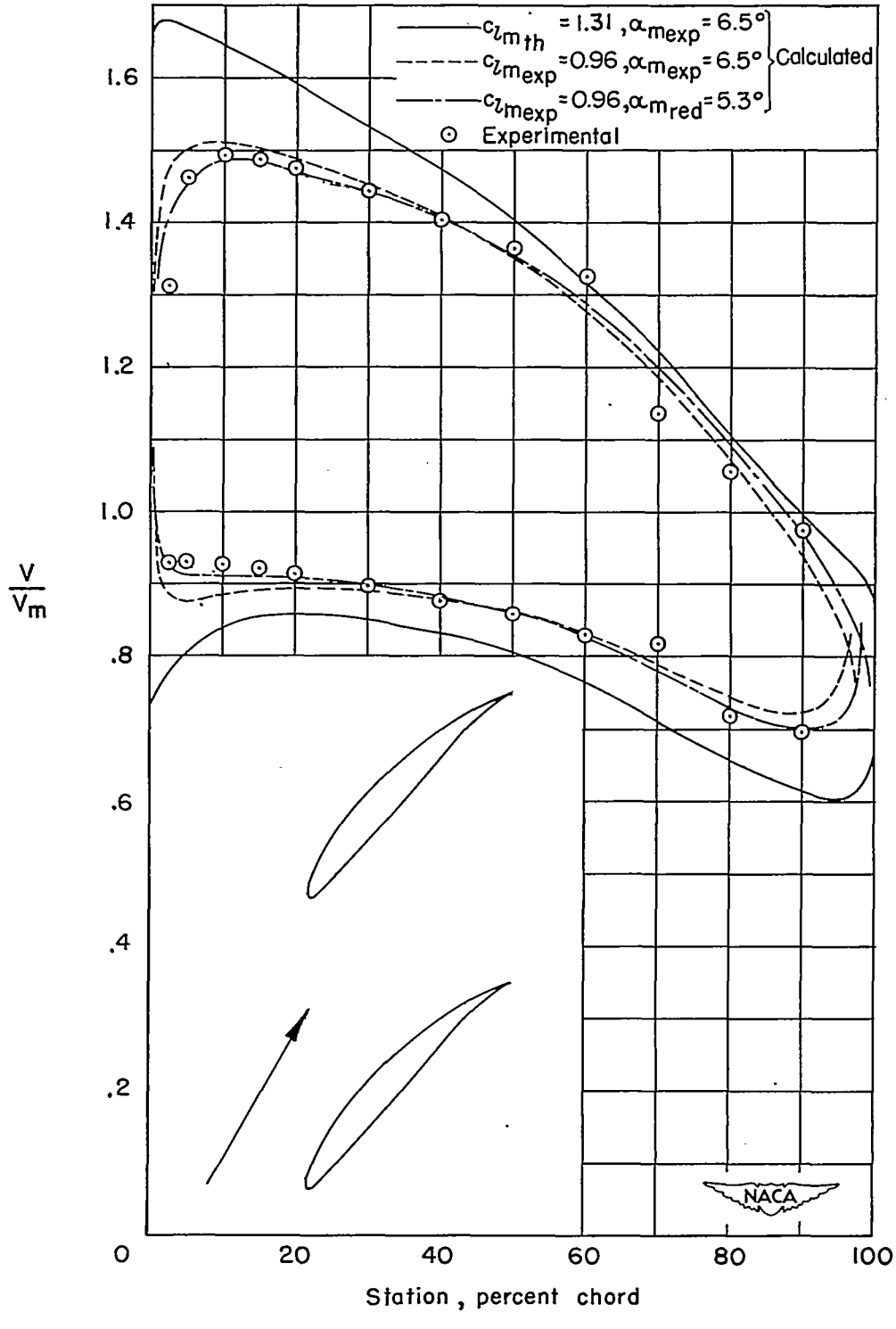

Figure 4.- Comparison of experimental and theoretical velocity distribution on airfoil in cascade. NACA 65-(12)10 airfoil; $\beta_1 = 60°$; $\alpha_1 = 14.1°$; $\alpha_m = 6.5°$; $\theta = 18.6°$; $\sigma = 1.0$.

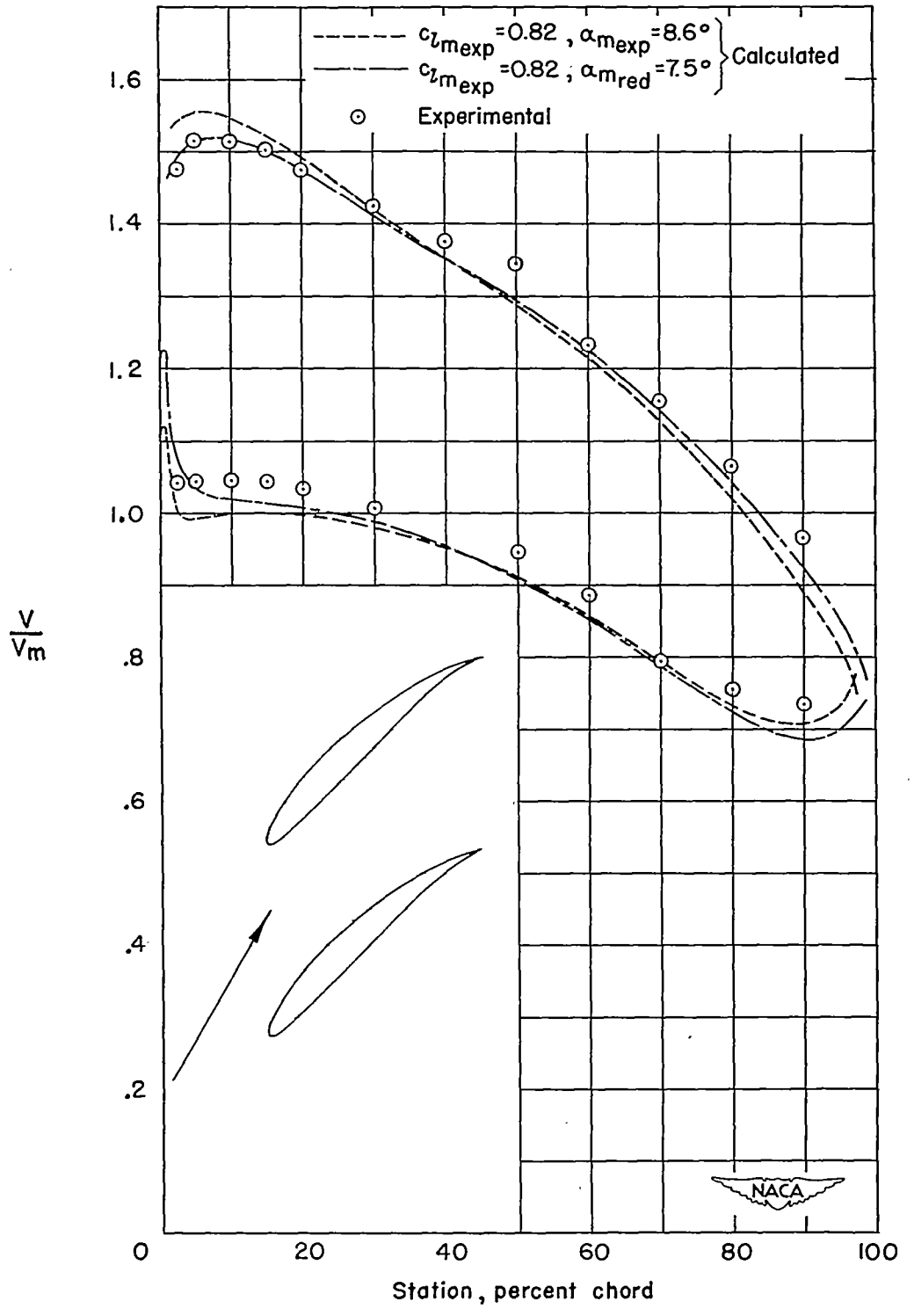

Figure 5.- Comparison of experimental and theoretical velocity distribution on airfoil in cascade. NACA 65-(12)10 airfoil; $\beta_1 = 60^\circ$; $\alpha_1 = 18.1^\circ$; $\alpha_m = 8.6^\circ$; $\theta = 24.6^\circ$; $\sigma = 1.5$.

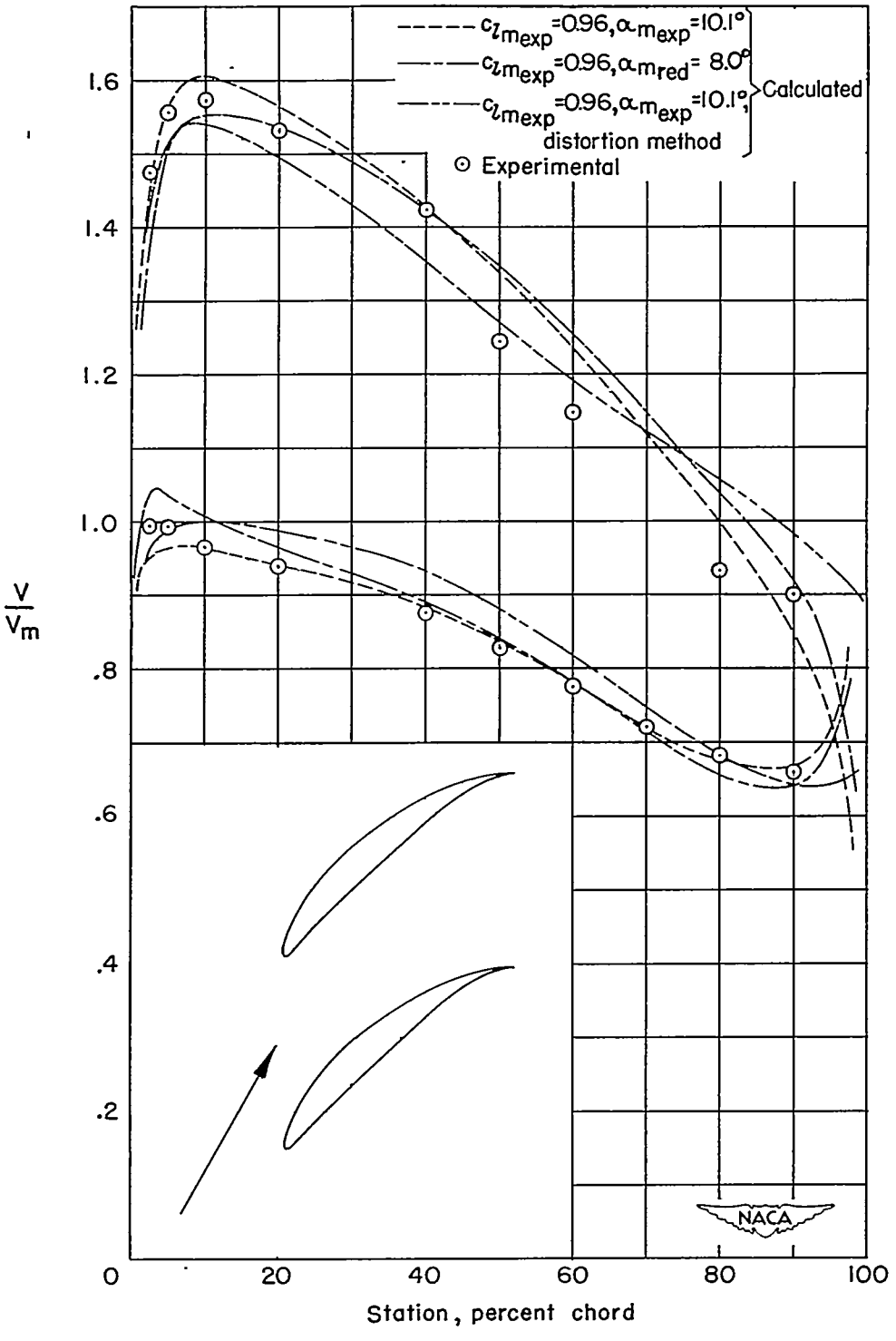

Figure 6.- Comparison of experimental and theoretical velocity distribution on airfoil in cascade. NACA 65-(18)10 airfoil; $\beta_1 = 60°$; $\alpha_1 = 21.0°$; $\alpha_m = 10.1°$; $\theta = 29.8°$; $\sigma = 1.5$.

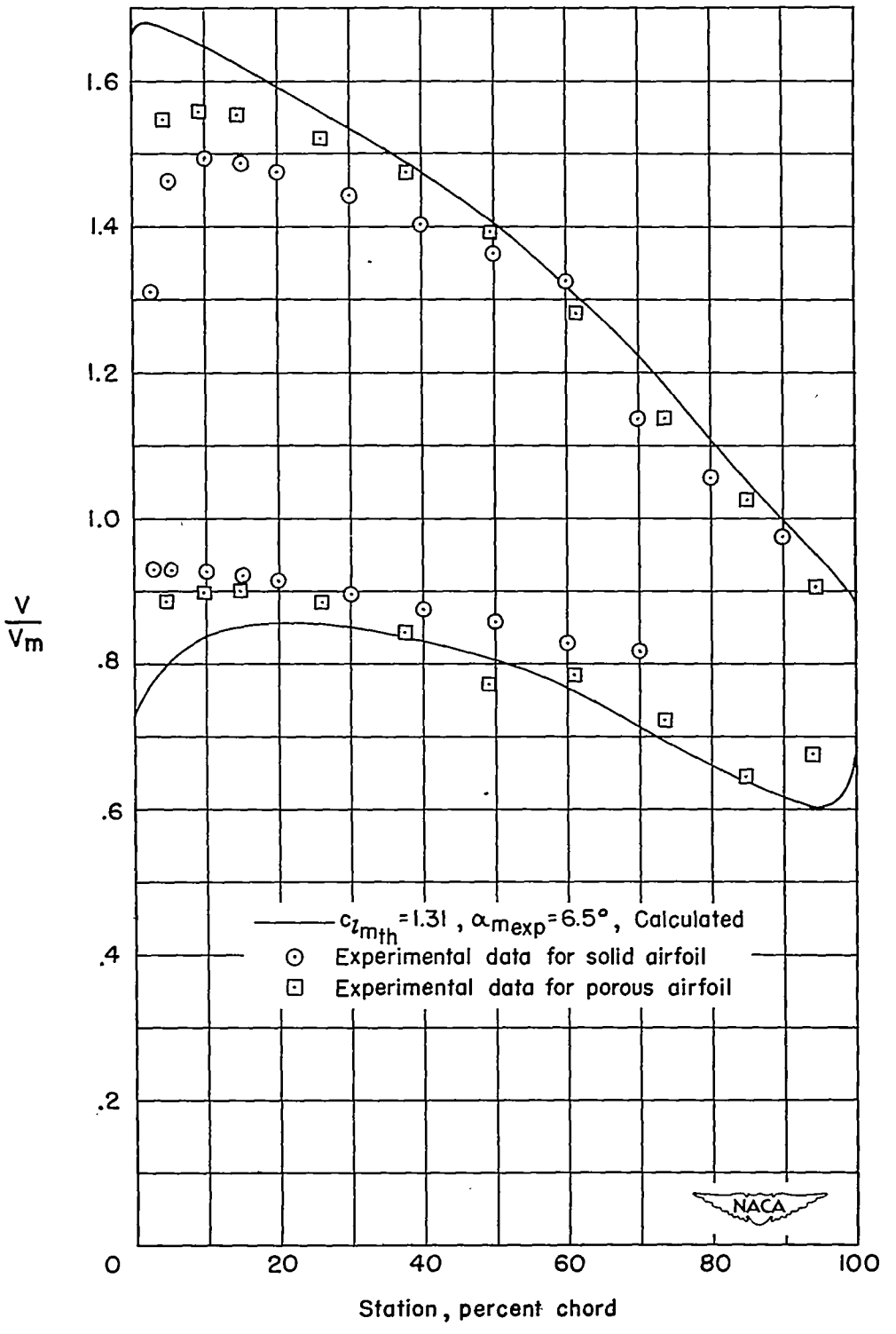

Figure 7.- Comparison of solid- and porous-surface cascade blades. NACA 65-(12)10 airfoil; $\beta_1 = 60°$; $\alpha_1 = 14.1°$ and $14.5°$; $\sigma = 1.0$.

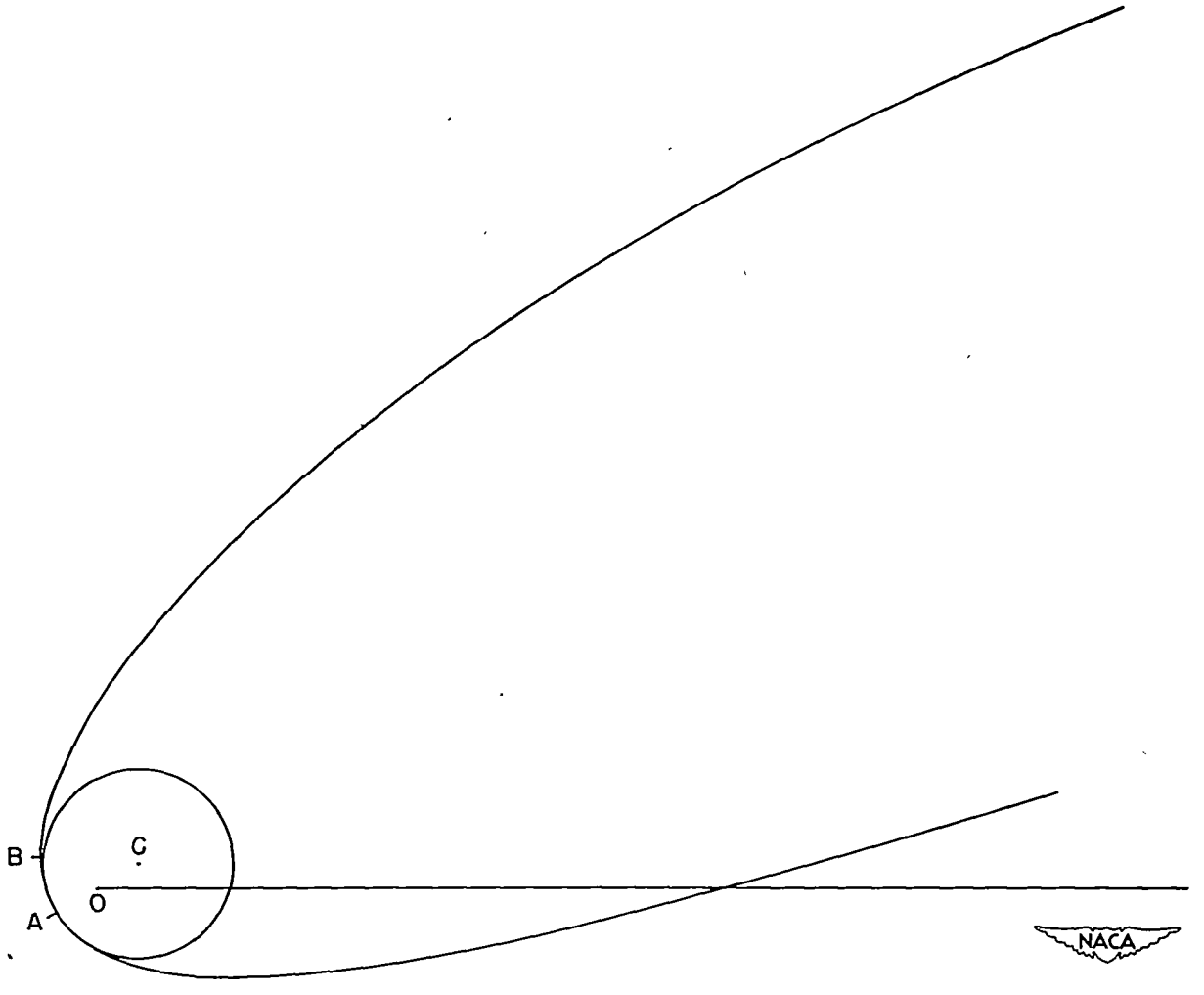

Figure 8.- Forward 30 percent of a highly cambered Joukowski airfoil. Point O is the tip of the reference axis (the line into which the unit circle is transformed). Point A is the end of the mean camber line and the point of minimum radius of curvature. Point B is the nominal leading edge, or farthest forward point. Point C is the center of curvature of the profile at point A.

NACA-Langley - 8-21-51 - 1000